

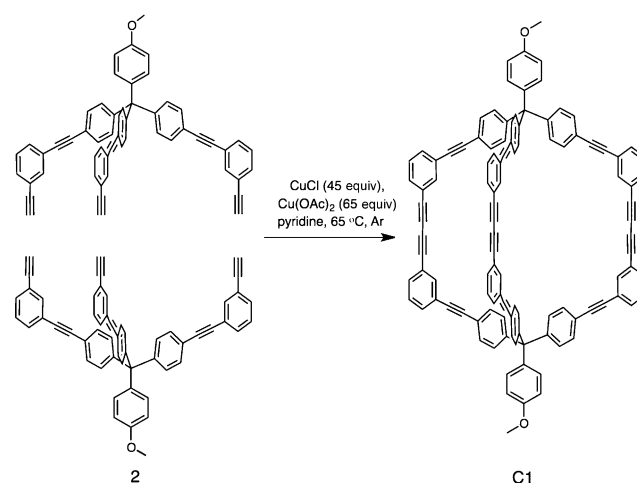
# Kinetically Controlled Porosity in a Robust Organic Cage Material\*\*

Antonio Avellaneda, Peter Valente, Alexandre Burgun, Jack D. Evans, Adrian W. Markwell-Heys, Damien Rankine, David J. Nielsen, Matthew R. Hill, Christopher J. Sumby,\* and Christian J. Doonan\*

Microporous materials are of significant interest owing to their central role in gas storage, separation processes, and catalysis.<sup>[1–4]</sup> Recently, microporous molecular solids composed of discrete, shape-persistent organic cages have received growing attention<sup>[1]</sup> because they possess unique properties that set them apart from conventional, extended network materials, such as zeolites,<sup>[2]</sup> metal–organic frameworks,<sup>[3]</sup> and covalent organic frameworks.<sup>[4]</sup> For example, molecular solids are readily solution-processable,<sup>[5]</sup> provide facile access to multicomponent materials by mix-and-match synthesis,<sup>[6]</sup> and, by virtue of their noncovalent intermolecular packing, can exhibit advanced properties, such as adsorbate-triggered on/off porosity switching.<sup>[7]</sup>

Unlike extended networks, where solvent-accessible voids are linked through rigid covalent framework solids composed of discrete organic cages predominantly aggregate by relatively weak dispersion forces. Predicting the crystal structures of such weakly aggregating materials is a long-standing challenge in solid-state chemistry,<sup>[8]</sup> and is, in this field, inherently coupled to estimating the ultimate porosity of a molecular solid from its building units, as different polymorphs can afford solids with dramatically different surface areas.<sup>[9]</sup> Accordingly, relatively few examples of porous organic solids have been reported.<sup>[1d]</sup> Nevertheless, recent work from the laboratories of Cooper and Mastalerz have demonstrated that the porosity of such materials can be modified through crystal engineering strategies and synthetic processing.<sup>[5a,10]</sup> Herein we describe the synthesis and characterization of a novel, permanently porous, shape-persistent

cage molecule (**C1**) that is constructed entirely from thermodynamically robust carbon–carbon bonds and has the molecular formula  $C_{112}H_{62}O_2$  (Scheme 1). Furthermore, we demonstrate kinetically controlled access to two crystalline polymorphs **C1 $\alpha$**  and **C1 $\beta$**  that possess dramatically different  $N_2$  porosities: polymorph **C1 $\alpha$** , which is nonporous to  $N_2$ , and polymorph **C1 $\beta$** , which affords a BET surface area of  $1153\text{ m}^2\text{ g}^{-1}$ .



**Scheme 1.** Procedure for the synthesis of trigonal-prismatic cage **C1**.

Molecule **C1** was synthesized by Eglinton homocoupling of two rigid, alkyne-terminated building units (Scheme 1; **2**). Such reactions, which are often conducted with a stoichiometric excess of copper reagents, have been widely employed in macrocycle synthesis.<sup>[11]</sup> The cage precursor, compound **2**, can be elaborated from a tripodal building block, 4-[tris(4-iodophenyl)methyl]phenol,<sup>[12]</sup> by sequential phenol methylation, Sonogashira coupling, and silyl deprotection reactions in 53% yield over three steps.<sup>[13]</sup> The ultimate homocoupling step proceeds under high-dilution conditions with a large excess of catalyst to maximize the yield of the kinetic product **C1**. The yield of **C1** (20%) is remarkable given the irreversible nature of the bonding involved and the fact that one incorrect bond formation step during cage synthesis will direct the reaction towards the formation of oligomers. No other major products are isolated in this reaction that requires three Eglinton homocoupling reactions. The energy-minimized structure of **C1** is best described as a distorted triangular prism with internal vertical and horizontal diameters of 13.5 Å and 12 Å, respectively.<sup>[14]</sup>

[\*] Dr. A. Avellaneda, Dr. P. Valente, Dr. A. Burgun, J. D. Evans, A. W. Markwell-Heys, D. Rankine, Dr. C. J. Sumby, Dr. C. J. Doonan School of Chemistry and Physics, The University of Adelaide Adelaide, South Australia, 5005 (Australia)  
E-mail: christian.doonan@adelaide.edu.au

Dr. D. J. Nielsen  
Human Protection and Performance Division  
Defence Science and Technology Organisation  
506 Lorimer St, Fishermans Bend, Victoria, 3207 (Australia)

Dr. M. R. Hill  
CSIRO, Materials Science and Engineering  
Private Bag 33, Clayton South MDC, Victoria 3169 (Australia)

[\*\*] C.J.D. and C.J.S. would like to acknowledge the Australian Research Council for funding (DP 120103909 (C.J.D.) and FT 100100400 (C.J.D.), and FT0991910 (C.J.S.)). D.J.N. and C.J.D. acknowledge support from the DSTO Fellowship programme. J.D.E. thanks CSIRO Materials Science and Engineering for a top-up Ph.D. scholarship.

Supporting information for this article is available on the WWW under <http://dx.doi.org/10.1002/anie.201209922>.

The most common strategy used to synthesize organic cages is to employ covalent dynamic imine chemistry to facilitate isolation of the thermodynamic molecular product from a one-step reaction. Inspired by analogous chemistry,<sup>[15]</sup> we aimed to expand the reaction space of such porous molecular solids by synthesizing a thermodynamically robust shape-persistent cage molecule by homocoupling of a single component. Furthermore, we note that the one-step synthesis of related multicomponent cages may be possible, under such bond-forming conditions, by judicious choice of templating strategies.<sup>[16]</sup>

The formation of **C1** was confirmed by <sup>1</sup>H NMR and <sup>13</sup>C NMR spectroscopy, which showed aromatic resonances in the range 7.76–6.85 ppm and a resonance for the methoxy group at 3.83 ppm in the <sup>1</sup>H NMR spectrum; these are all consistent with the cage structure.<sup>[13]</sup> The alkyne proton of **2** is notably absent from the <sup>1</sup>H NMR spectrum of **C1**, and electrospray ionization mass spectrometry (ESI-MS) showed a peak for the parent ion at *m/z* 1439, which corresponds to [**C1**]<sup>+</sup>. Two weak IR bands for the C≡C stretches at 2219 and 2207 cm<sup>-1</sup> were readily apparent. Bulk samples of **C1** were readily desolvated and stable up to about 400 °C, as determined by concomitant thermal gravimetric analysis–differential scanning calorimetry (TGA-DSC) experiments. It is noteworthy that the DSC trace showed no evidence of chemical transformations below 400 °C. This is quite remarkable given the close proximity of three diyne moieties but points to the overall rigidity and thermal robustness of the structure. **C1** is soluble in common organic solvents, such as

chloroform, dichloromethane, and benzene, but insoluble in alcohols, H<sub>2</sub>O, and other highly polar solvents.

Large colorless block-shaped crystals of **C1** formed in approximately 24 h from slow evaporation of a dichloromethane/methanol solution of **C1**. The crystal structure of **C1**<sup>[17]</sup> (Figure 1) closely resembles the energy-minimized structure identified by computational approaches. The vertical and horizontal outer dimensions of **C1** are circa 3.1 nm by 1.6 nm, and these enclose an internal cavity of the dimensions noted. The volume occupied by a cage molecule is about 1300 Å<sup>3</sup>. The preorganized tripodal building block adopts the geometry anticipated from initial modeling and structure prediction with angles of 104.1(3)–111.5(3)° around the tetraphenyl carbon atom. The dialkynyl struts are close to linear and all alkyne moieties have the expected bond lengths (in the range 1.171(5)–1.224(5) Å). This single-crystalline polymorph, **C1α**, crystallizes in the orthorhombic space group *Pbcn* with four molecules in the unit cell. Consideration of the packing reveals that the cages pack in a herringbone-type arrangement, if the cages are treated as rods along their long molecular axis. Each individual molecule of **C1** packs closely with four other molecules of **C1** in the same orientation and two sets of four additional cages, with a near-orthogonal direction of their molecular axis, at the poles of the first cage (Figure 1b). This has the effect of placing at least two molecules of **C1** into each window of an individual cage. Owing to the lack of functional groups directing the packing, the primary intercage forces in the crystal packing are van der Waals interactions and edge-to-face  $\pi$ -stacking interactions

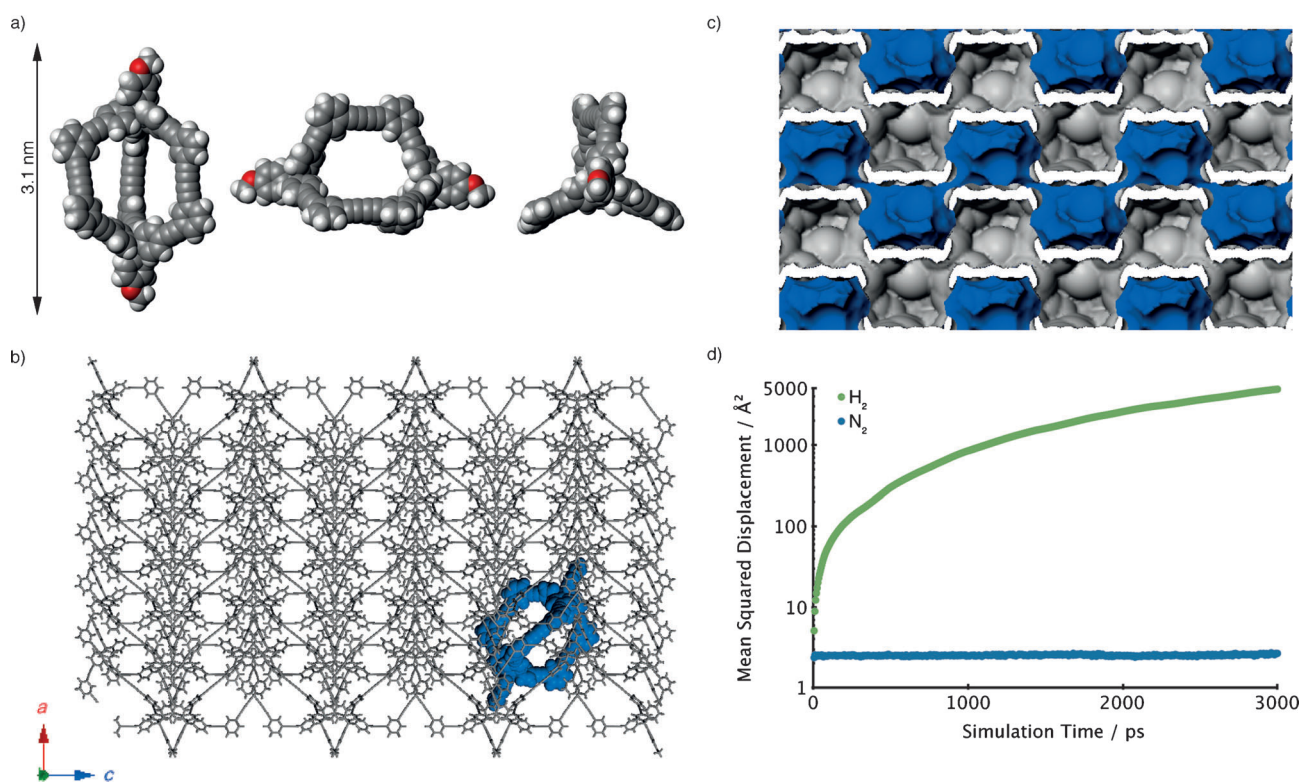


**Figure 1.** a) Representations of the structure of **C1** and b) wire-framed depiction of the packing of **C1α** down the *b* axis. c) N<sub>2</sub> accessible surface area of **C1α** and d) the simulated mean-squared displacement of N<sub>2</sub> and H<sub>2</sub> through **C1α**.

involving both phenyl and alkyne moieties.<sup>[18]</sup> The crystals of **C1** contain residual solvent electron density peaks that could not be definitively identified and the SQUEEZE routine of Platon<sup>[19]</sup> was applied to the collected data.<sup>[20]</sup> Powder X-ray diffraction (PXRD) was used to confirm that the single crystal structure was representative of the bulk sample and determine that the  $\alpha$  polymorph was retained subsequent to evacuation of residual solvent.<sup>[13]</sup>

The simulated accessible pore space of  $N_2$  displayed in Figure 1c shows that the structure of **C1 $\alpha$**  contains one-dimensional channels comprised of adjacent cages connected by windows of about 4 Å. Given that the kinetic diameter of  $N_2$  is 3.64 Å<sup>[21]</sup> it was expected that these windows would restrict the diffusion of  $N_2$  through the material. To support this hypothesis we employed molecular dynamics to simulate the diffusion of  $H_2$  and  $N_2$  within the pore structure of **C1 $\alpha$** .<sup>[22]</sup> This was determined by measuring the mean-square displacement of single  $N_2$  and  $H_2$  molecules for 3 ns after 1 ns of equilibration at 77 K. Figure 1d clearly shows that the motion of  $N_2$  is constrained within polymorph **C1 $\alpha$**  while the smaller  $H_2$  is able to diffuse through the structure by the circa 4 Å windows. In accordance with these structure simulations, 77 K  $N_2$  isotherms indicated that activated samples of **C1 $\alpha$**  were non-porous to  $N_2$  but porous to  $H_2$ , affording a total uptake of approximately  $40 \text{ cm}^3 \text{ g}^{-1}$  at 77 K. However, **C1 $\alpha$**  can be considered a “soft” porous crystal, and it is plausible that with greater gas loading pressures and temperature, slight structural deformations may allow  $N_2$  to diffuse through the framework.

Rapid precipitation of **C1** was found to reliably form a second, kinetically trapped polymorph **C1 $\beta$** . Addition of an antisolvent to solutions of **C1** or freeze drying from benzene both form microcrystalline powders with identical PXRD patterns (Figure 2). Upon solvent removal and drying, polymorph **C1 $\beta$**  retains crystallinity and yields a PXRD pattern that corresponds to the solvated forms, indicating structural uniformity subsequent to guest removal. The propensity of **C1** to form a crystalline material following

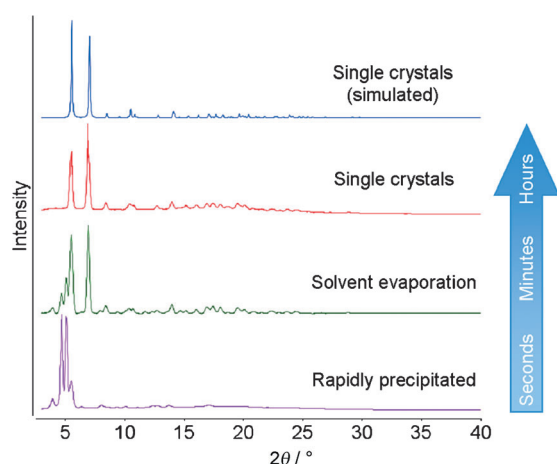


**Figure 2.** PXRD patterns of desolvated samples of **C1 $\alpha$**  (red) and **C1 $\beta$**  (mauve). The green PXRD pattern shows a mixture of polymorphs **C1 $\alpha$** , and **C1 $\beta$** . The blue arrow on the right of the Figure is a guide for the timescale in which each solid sample was crystallized.

freeze drying is very unusual for porous molecular solids, however, we note that PXRD methods are silent to the presence of an amorphous component. Scanning electron microscopy (SEM) indicated that polymorph **C1 $\beta$**  forms thin plate-like crystallites, in contrast to polymorph **C1 $\alpha$**  that form block-shaped crystals.<sup>[13]</sup> This plate-like morphology of the **C1 $\beta$**  polymorph accounts for the broadness of the peaks and weak high-angle diffraction in the PXRD. Our contention that access to crystalline polymorphs **C1 $\alpha$**  and **C1 $\beta$**  is a kinetically driven process is supported by PXRD experiments carried out on samples of **C1** generated from supersaturated solutions on a rotary evaporator (Figure 2). Solvent evaporation from a solution of **C1** in dichloromethane gives rise to crystalline solids with PXRD patterns that are consistent with a mixture of both polymorphs. On the qualitative time scales investigated in this work, solvent evaporation (minutes) lies in the intermediate range between single crystal growth by slow evaporation (hours to days) and rapid precipitation (seconds). We acknowledge that exploration of other crystallization techniques, solvent combinations, and temperatures may provide access to additional polymorphs. Nevertheless, we clearly demonstrate predictable and reproducible access to polymorphs **C1 $\alpha$**  and **C1 $\beta$**  by simple kinetic control. These observations suggest that crystallization of **C1** follows Ostwald's rule, as **C1 $\beta$**  is kinetically trapped in a metastable crystalline phase that upon dissolution and slow crystallization affords the thermodynamically favored form **C1 $\alpha$** .<sup>[23]</sup> Although the formation of **C1 $\alpha$**  and **C1 $\beta$**  is kinetically driven, variable-temperature PXRD experiments showed no evidence that a thermodynamic phase transition occurs in the solid state.

We assessed the permanent porosity of polymorph **C1 $\beta$**  by first evacuating solvent molecules from its pores (12 hours, 2  $\mu$ Torr, 298 K) and then measuring a  $N_2$  isotherm at 77 K (Figure 3). The isotherm shape is best described as type 1, which is consistent with pore diameters of less than 2 nm. The slight hysteric behavior suggests the presence of structural inhomogeneity or poor uniformity in crystal size distribution and this has been observed in other porous molecular solids and flexible metal–organic framework materials.<sup>[10a]</sup> BET analysis of the isotherm in Figure 3 indicates that **C1 $\beta$**  has a surface area of  $1153 \text{ m}^2 \text{ g}^{-1}$ . It is noteworthy that surface areas in excess of  $1000 \text{ m}^2 \text{ g}^{-1}$  are rare for molecular cages.<sup>[1]</sup> Additionally, polymorph **C1 $\beta$**  can be dissolved and precipi-

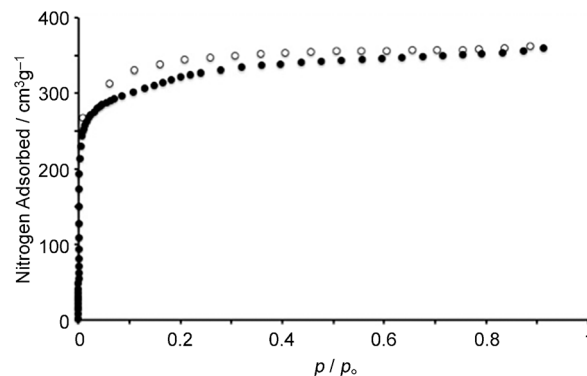


**Figure 3.**  $N_2$  77 K isotherm of **C1 $\beta$** . ● adsorption, ○ desorption.

tated several times without diminishing the accessible surface area. These properties highlight the facile processability of **C1**. Pore size distributions calculated by nonlocal density functional theory from the adsorption data shows two main peaks centered at approximately 6 Å and 11 Å. The larger pore size corresponds well to the predicted internal pore diameter of **C1** and the presence of a second pore suggests solvent accessible extrinsic voids. However, in the absence of structural data, the contribution of intrinsic and extrinsic porosity to the total surface area cannot be confirmed.

In summary, we have described the synthesis and characterization of a robust organic cage that is constructed entirely from carbon-carbon bonds. Solids of **C1** can be predictably crystallized by kinetic control into two separate polymorphs **C1 $\alpha$**  and **C1 $\beta$** . Rapid precipitation of **C1** leads to the permanently porous polymorph **C1 $\beta$** , which has a notably high surface area of 1153 m<sup>2</sup>g<sup>-1</sup> for a molecular solid; however, slow crystallization methods yield **C1 $\alpha$** , which was found to be nonporous to N<sub>2</sub> gas. Such control of polymorphism is of great interest, as the properties of polymorphic materials can, as in this present case, show remarkable variation. Furthermore, fine control of polymorphism can provide insight into the mechanism of multistage polymorphic transitions from the beginning of crystallization to the formation of stable solids. We are currently investigating if the kinetic trapping methods observed in this work can be generally applied to derivatives of **C1**. Additionally, we are also synthesizing **C1** analogues functionalized with moieties designed to enhance its selective gas adsorption properties.

Received: December 12, 2012

Published online: ■ ■ ■ ■, ■ ■ ■ ■ ■ ■

**Keywords:** cage compounds · crystallization landscapes · kinetic control · polymorphism · porosity

- [1] a) J. R. Holst, A. Trewin, A. I. Cooper, *Nat. Chem.* **2010**, *2*, 915; b) A. I. Cooper, *Angew. Chem.* **2011**, *123*, 1028; *Angew. Chem. Int. Ed.* **2011**, *50*, 996; c) M. Mastalerz, *Angew. Chem.* **2010**, *122*, 5164; *Angew. Chem. Int. Ed.* **2010**, *49*, 5042; d) M. Mastalerz, *Chem. Eur. J.* **2012**, *18*, 10082.
- [2] M. E. Davis, *Nature* **2002**, *417*, 813.
- [3] a) M. Eddaoudi, J. Kim, N. Rosi, D. Vodak, J. Wachter, M. O’Keeffe, O. M. Yaghi, *Science* **2002**, *295*, 469; b) J. L. C. Rowsell, O. M. Yaghi, *Microporous Mesoporous Mater.* **2004**, *73*, 3; c) S. Kitagawa, R. Kitaura, S. Noro, *Angew. Chem.* **2004**, *116*, 2388; *Angew. Chem. Int. Ed.* **2004**, *43*, 2334; d) O. K. Farha, J. T. Hupp, *Acc. Chem. Res.* **2010**, *43*, 1166.
- [4] a) A. P. Côté, A. I. Benin, N. W. Ockwig, A. J. Matzger, M. O’Keeffe, O. M. Yaghi, *Science* **2005**, *310*, 1166; b) H. M. El-Kaderi, J. R. Hunt, J. L. Mendoza-Cortés, A. P. Côté, R. E. Taylor, M. O’Keeffe, O. M. Yaghi, *Science* **2007**, *316*, 268; c) F. J. Uribe-Romo, J. R. Hunt, H. Furukawa, C. Klock, M. O’Keeffe, O. M. Yaghi, *J. Am. Chem. Soc.* **2009**, *131*, 4570; d) J. R. Hunt, C. J. Doonan, J. D. LeVangie, A. P. Côté, O. M. Yaghi, *J. Am. Chem. Soc.* **2008**, *130*, 11872; e) F. J. Uribe-Romo, C. J. Doonan, H. Furukawa, K. Oisaki, O. M. Yaghi, *J. Am. Chem. Soc.* **2011**, *133*, 11478.
- [5] a) T. Hasell, S. Y. Chong, K. E. Jelfs, D. J. Adams, A. I. Cooper, *J. Am. Chem. Soc.* **2012**, *134*, 588; b) T. Hasell, A. I. Cooper, *Adv. Mater.* **2012**, *24*, 5732.
- [6] a) S. Jiang, J. T. A. Jones, T. Hasell, C. E. Blythe, D. J. Adams, A. Trewin, A. I. Cooper, *Nat. Commun.* **2011**, *2*, 207; b) T. Hasell, S. Y. Chong, M. Schmidtman, D. J. Adams, A. I. Cooper, *Angew. Chem.* **2012**, *124*, 7266; *Angew. Chem. Int. Ed.* **2012**, *51*, 7154.
- [7] J. T. A. Jones, D. Holden, T. Mitra, T. Hasell, D. J. Adams, K. E. Jelfs, A. Trewin, D. J. Willock, G. M. Day, J. Bacsá, A. Steiner, A. I. Cooper, *Angew. Chem.* **2011**, *123*, 775; *Angew. Chem. Int. Ed.* **2011**, *50*, 749.
- [8] G. R. Desiraju, *Nat. Mater.* **2002**, *1*, 77.
- [9] T. Tozawa, J. T. A. Jones, S. I. Swamy, S. Jiang, D. J. Adams, S. Shakespeare, R. Clowes, D. Bradshaw, T. Hasell, S. Y. Chong, C. Tang, S. Thompson, J. Parker, A. Trewin, J. Basca, A. M. Z. Slawin, A. Steiner, A. I. Cooper, *Nat. Mater.* **2009**, *8*, 973.
- [10] a) M. J. Bojdys, M. E. Briggs, J. T. A. Jones, D. J. Adams, S. Y. Chong, M. Schmidtman, A. I. Cooper, *J. Am. Chem. Soc.* **2011**, *133*, 16566; b) M. W. Schneider, I. M. O’Connell, H. Ott, L. G. Lechner, H.-J. S. Hauswald, R. Stoll, M. Mastalerz, *Chem. Eur. J.* **2012**, *18*, 836.
- [11] a) J. J. Li, *Name Reactions: A Collection of Detailed Mechanisms and Synthetic Applications*, Springer, Berlin, **2009**; b) H. A. Stefani, A. S. Guarezemini, R. Cella, *Tetrahedron* **2010**, *66*, 7871.
- [12] M. E. Gallina, B. Baytekin, C. Schalley, P. Ceroni, *Chem. Eur. J.* **2012**, *18*, 1528.
- [13] See the Supporting Information for full experimental details.
- [14] The structure of **C1** was optimized to B3LYP/6-31G(d,p) theory with default convergence criteria. The vertical diameter was measured between the two sp<sup>3</sup> carbon atoms of the cage framework and the horizontal diameter was defined as twice the average distance between the cage centroid and the diyne moiety. Full reference to these methods is in the Supporting Information.
- [15] a) C. Zhang, C.-F. Chen, *J. Org. Chem.* **2007**, *72*, 9339; b) C. Zhang, Q. Wang, H. Long, W. Zhang, *J. Am. Chem. Soc.* **2011**, *133*, 20995.
- [16] a) R. L. E. Furlan, S. Otto, J. K. M. Sanders, *Proc. Natl. Acad. Sci. USA* **2002**, *99*, 4801; b) C. D. Meyer, C. S. Joiner, J. F. Stoddart, *Chem. Soc. Rev.* **2007**, *36*, 1705.
- [17] Selected data for **C1**: C<sub>112</sub>H<sub>62</sub>O<sub>2</sub>, *M<sub>r</sub>* 1439.72, *T* = 150(2) K, orthorhombic, *Pbcn*,  $\alpha = 31.9812(14)$ ,  $\beta = 18.5193(8)$ ,  $\gamma = 20.3265(7)$  Å, *V* = 12038.8(8) Å<sup>3</sup>, *Z* = 4,  $\rho_{\text{calc.}} = 0.794$  Mg m<sup>-3</sup>,  $\mu = 0.046$  mm<sup>-1</sup>, *F*(000) 3000, colorless block, 0.33 × 0.31 × 0.06 mm<sup>3</sup>, 56266 reflections collected, 14052 independent reflections [*R*<sub>int</sub> = 0.1347], completeness 99.9%, data/restraints/parameters 14052/0/515, GOF 0.871, *R*<sub>1</sub> = 0.0888, *wR*<sub>2</sub> = 0.2291, (all data: *R*<sub>1</sub> = 0.2581, *wR*<sub>2</sub> = 0.2839). CCDC 913184 contains the supplementary crystallographic data for this paper. These data can be obtained free of charge from The Cambridge Crystallographic Data Centre via www.ccdc.cam.ac.uk/data\_request/cif.
- [18] S. Dawn, M. B. Dewal, D. Sobransingh, M. C. Paderes, A. C. Wibowo, M. D. Smith, J. A. Krause, P. J. Pellechia, L. S. Shimizu, *J. Am. Chem. Soc.* **2011**, *133*, 7025.
- [19] A. L. Spek, *Acta Crystallogr. Sect. D* **2009**, *65*, 148.
- [20] The SQUEEZE routine of PLATON was applied to the collected data, which resulted in significant reductions in *R*<sub>1</sub> and *wR*<sub>2</sub> and an improvement in the GOF. *R*<sub>1</sub>, *wR*<sub>2</sub> and GOF before SQUEEZE routine: 18.6%, 52.4% and 1.22; after SQUEEZE routine: 8.88%, 28.4% and 0.87.
- [21] L. M. Robeson, *J. Membr. Sci.* **1991**, *62*, 165–185.
- [22] T. X. Nguyen, S. K. Bhatia, *J. Phys. Chem. C* **2007**, *111*, 2212.
- [23] T. Threlfall, *Org. Process Res. Dev.* **2003**, *7*, 1017.

## Communications



### Porous Molecular Solids

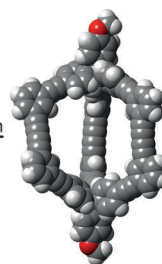
A. Avellaneda, P. Valente, A. Burgun,  
J. D. Evans, A. W. Markwell-Heys,  
D. Rankine, D. J. Nielsen, M. R. Hill,  
C. J. Sumby,\*  
C. J. Doonan\* ————— ■■■■-■■■■

Kinetically Controlled Porosity in a Robust  
Organic Cage Material



Non-Porous

← Slow Crystallization



→ Rapid Precipitation



Porous

**Won by the hare:** A new crystalline microporous solid was prepared that is composed of discrete organic cages made entirely from carbon-carbon

bonds. The porosity of this material can be controlled by simple kinetic methods, which afford reproducible access to either a non-porous or porous polymorph.